CUPID Code Simulation of Two-Dimensional Film Flow Test

Y. J. Cho[a*], H. Y. Yoon[a], J. H. Yang[a,b], and H. K. Cho[b]
[a]*Korea Atomic Energy Research Institute, 111 Daedeok-daero, 989 Beon-gil, Yuseong-gu, Daejeon 305-600*
[b]*Nuclear Thermal-Hydraulic Eng. Lab. Seoul Nat. Univ. Gwanak 599, Gwanak-ro, Gwanak-gu, Seoul 151-742*
[*]*Corresponding author: yjcho@kaeri.re.kr*

1. Introduction

CUPID1.8 (Component Unstructured Program for Interfacial Dynamics 1.8) code has been developed for a high-resolution analysis of two-phase flows in nuclear components in KAERI [1]. Since the CUPID code has been developed, various verification and validation (V&V) problems have been solved to confirm not only the numerical stability, robustness and accuracy, but also the adequacy of physical models in the CUPID code [2].

Recently, the verification test has being performed for an interfacial drag and wall shear stress models. The interfacial friction plays an important role in two-phase flow problems such as a horizontally stratified flow in cold legs, free surface in a large pool, liquid film flow in a downcomer, and so on.

During the reflood phase in the large break loss of coolant accident (LBLOCA), the interaction between the falling liquid film and the steam flow induces a two-phase multi-dimensional film flow when the emergency core coolant is injected into the upper downcomer. In this case, the wall shear force also affect the thickness and shape of liquid film.

Two-dimensional film flow experiments performed at the Korea Atomic Energy Research Institute (KAERI) were used to verify the wall shear and interfacial drag models in the CUPID1.8 code. The sensitivity of the each model on the film flow was also numerically investigated.

2. Two-dimensional Film Flow Experiments

2.1 Description of Experimental Facility

KAERI constructed a two-phase film flow experimental facility to investigate the behavior of falling liquid film interacting with a laterally blowing air flow, as shown in Fig. 1 [3]. The facility consists of a test section made by parallel acrylic plates, a water supply system, and an air supply system.

Air was used instead of steam to separate the condensation effect from the hydraulic effect. The air was injected into the 6-inch pipe through a perforated plate in the expansion section for a uniform flow distribution. Water with fluorescent particles for PIV was injected through a 1-inch nozzle. The injected water impinged on the test section wall (1.4 m x 0.62 m x 0.025 m) and fell down on the flat plate wall. The injected air and fallen water were divided by a separator after an interaction in the test section.

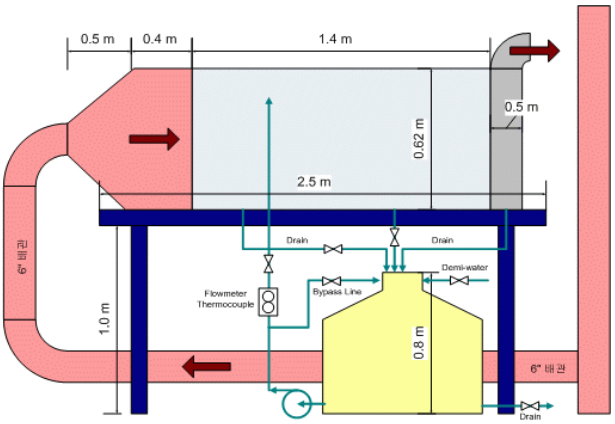

Fig. 1. Schematic of two-dimensional film flow experimental facility

2.2. Test Condition and Measurements

The test section was reduced by a scaling ratio of 1/10 against the APR1400. According to the linear scaling method, the velocity was scaled down by the square root of the scaling ratio. Therefore, the inlet liquid velocity and air velocity were reduced to 0.63 m/s from 2 m/s and to 5 – 15 m/s from 15 – 45 m/s.

To measure the liquid film velocity, a volume-PIV method using 1 to 20 ㎛ particles was applied. The control volume was divided into 19x7 sub-grids to make the field of view for a high-speed camera, as shown in Fig. 2. The sub-grid has dimension of 30 mm x 30 mm.

Fig. 2. Control volume and sub-grids for measurements

The thickness of the liquid film was measured using a pulse-echo type ultrasonic thickness gauge.

3. Interfacial Drag Models in CUPID1.8

CUPID1.8 uses different interfacial drag models according to the topology map. Three topology regions are used, as shown in Fig. 3: the bubble topology, mist

topology, and sharp interface topology [4].

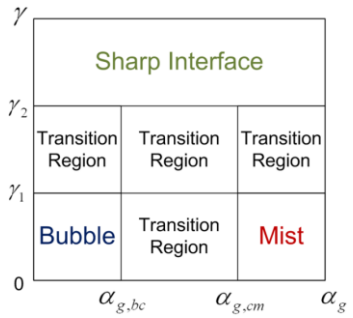

Fig. 3. Inter-phase topology map in CUPID1.8 code

If a sharp interface between a liquid and gas phase exists, such as a liquid film flow, a free surface in a large pool, and a horizontally stratified flow in the pipes, the drag force model for the sharp interface topology is the most sensitive factor for a stable calculation.

3.1 Bubble Topology

Interfacial drag force in a bubble topology map is expressed as

$$F_{gl} = \frac{1}{8} a_i \rho_l C_D |\vec{u}_g - \vec{u}_l| \quad (1)$$

$$\begin{cases} C_D = Max\left(0.44, \frac{24}{\mathrm{Re}_b}\left(1+0.15\mathrm{Re}_b^{0.687}\right)\right) & 0 < \mathrm{Re}_b \le 1000 \\ C_D = 0.44 & \mathrm{Re}_b > 1000 \end{cases} \quad (2)$$

where $\mathrm{Re}_b = \frac{\rho_l |\vec{u}_g - \vec{u}_l| D_b}{\mu_l}$.

3.2 Mist Topology

Interfacial drag force in a mist topology map is expressed as

$$F_{gl} = \frac{1}{8} a_i \rho_l C_D |\vec{u}_g - \vec{u}_l| \quad (3)$$

$$\begin{cases} C_D = Max\left(0.44, \frac{24}{\mathrm{Re}_d}\left(1+0.15\mathrm{Re}_d^{0.687}\right)\right) & 0 < \mathrm{Re}_d \le 1000 \\ C_D = 0.44 & \mathrm{Re}_d > 1000 \end{cases} \quad (4)$$

where $\mathrm{Re}_d = \frac{\rho_g |\vec{u}_g - \vec{u}_l| D_{drop}}{\mu_g}$.

3.3 Sharp Interface Topology

Interfacial drag force in a sharp interface topology map is expressed as

$$F_{gl} = \frac{1}{2} a_i \rho_g C_i(\varphi) |\vec{u}_g - \vec{u}_l| \quad (3)$$

$$C_i(\phi) = C_{i,\tan} + (C_{i,ort} - C_{i,\tan}) |\cos\phi| \quad (4)$$

where $C_{i,tan}$=0.005, $C_{i,ort}$=1.0, and $\cos\varphi = \frac{(\vec{u}_g - \vec{u}_l)\cdot\nabla\alpha}{|\vec{u}_g - \vec{u}_l||\nabla\alpha|}$.

4. Wall Shear Model in CUPID1.8

After the injected water impinges against the wall, it flows down and forms a thin liquid film. The thickness and velocity of liquid film strongly depend on the wall shear force as well as the interfacial drag force.

To acquire the wall shear force, the velocity profile in normal direction to the wall across the film is required. In the CUPID 1.8, the liquid velocity profile across the film is assumed as follows [5]

$$v(y) = v_w + \left(3\frac{v_f - v_w}{\delta_f} - \frac{\tau_{fs}}{2\mu}\right)y - \left(3\frac{v_f - v_w}{2\delta_f{}^2} - \frac{3\tau_{fs}}{4\mu\delta_f}\right)y^2 \quad (1)$$

where, $v_w, v_f, \tau_{fs} y$ are wall velocity, average film velocity, shear force at the film free surface, and local coordinate normal to the wall, respectively. In this model, the thin film is assumed to apply the laminar boundary layer approximation. Then, the wall shear stress can be calculated from Eq. (1) as

$$\tau_w = \mu_l \left(\frac{\partial v}{\partial y}\right)_{y=0} \quad (2)$$

In the calculation, the region where the thin liquid film exists is predefined as a user defined boundary condition.

4. CUPID1.8 Calculation

4.1 Grid Generation

The calculation grid was generated using a commercial grid generation tool, GiD, as shown in Fig. 4. A total of 81,464 grids were used to model the water injection nozzle and the rectangular test section. Other components were treated as boundary conditions including the air blower, air injection pipe, manifold structures, and separator connected to the outlet of the test section. Finer grids were used for the water injection nozzle and the specific part of the test section where the injected water impinges.

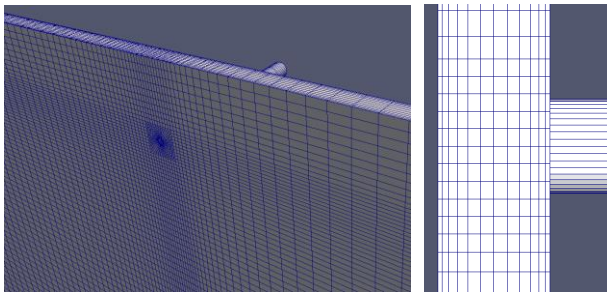

Fig. 4. Calculation grid for 2D film flow experimental facility

4.2 Initial and Boundary Conditions

The test case with the averaged air inlet velocity of

8.97 m/s, and the averaged water injection velocity of 0.63 m/s was selected as a base case. Velocity profile of the water injected from the water nozzle was assumed to be uniform. However, the pipe length of upstream is over 40 times of L/D so that the fully developed velocity profile can be achieved.

The velocity profile of air is applied as shown in Fig. 5 using the experimental data. This profile affect the local air velocity where the air interacts with the injected water plume and, consequently, the behavior of the liquid film.

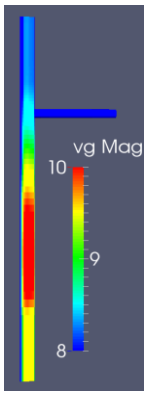

Fig. 5. Velocity profile of air at the inlet boundary

Atmospheric pressure and room temperature air was filled in the test section and water injection nozzle in the initial state.

4.3 Calculation Results

Fig. 6 shows the experimental data for the velocity distribution of the liquid film. The velocity vectors of liquid film generally head to the right direction due to the blowing air from the left boundary.

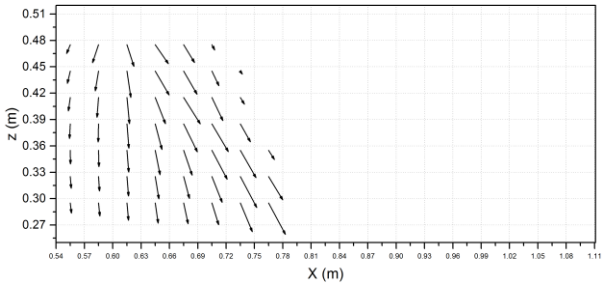

Fig. 6. Velocity distribution of liquid film (Experiment)

Fig. 7 and Fig. 8 show the calculation results without and with the wall shear model, respectively. By introducing the wall shear model, the thin liquid film in the lower region of the injection nozzle is simulated as highlighted with the red circle in Fig. 8. However, the velocity vector in the right region of the liquid film is still larger than the experimental data. This result means that the current wall shear model underestimates the wall shear force at the edge of the liquid film where the thickness of film is relatively thin. In addition, a droplet entrainment occurred in the experiment and caused the thin liquid film at the both side edges while this effect was not considered in the calculation.

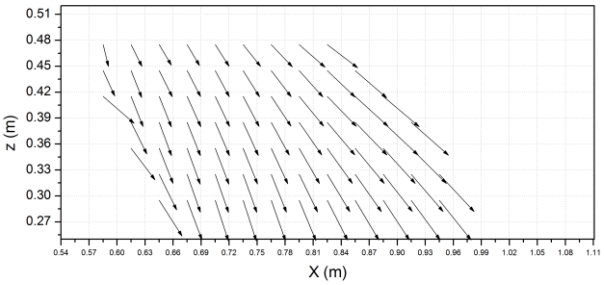

Fig. 7. Velocity distribution of liquid film (CUPID without wall shear model)

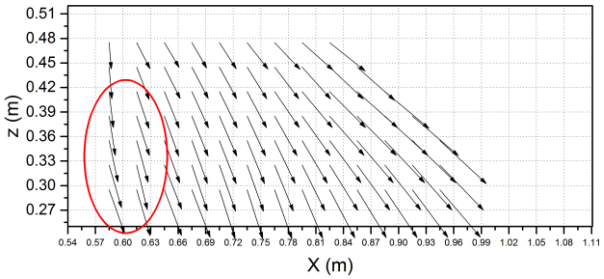

Fig.8. Velocity distribution of liquid film (CUPID with wall shear model)

The thickness of liquid film is compared in Fig 9 and Fig. 10. In the calculation, the wall shear model was applied. As shown in the figures, the order of film thickness is similar but the inclination and the width of the liquid film show some discrepancy.

From the comparison results of the velocity distribution and thickness of the liquid film, it can be concluded that the effect of interfacial drag force should increase in the region where the liquid film is thick. On the other hand, the wall shear force should become more effective and the droplet entrainment should be considered in the region where the liquid film is relatively thin.

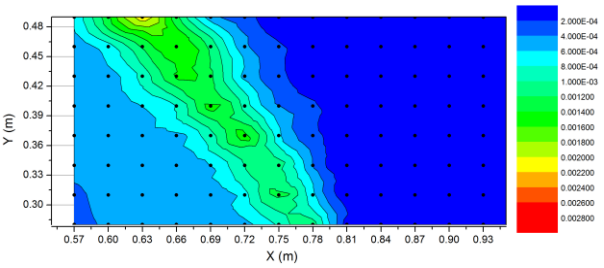

Fig. 9. Liquid film thickness (Experiment)

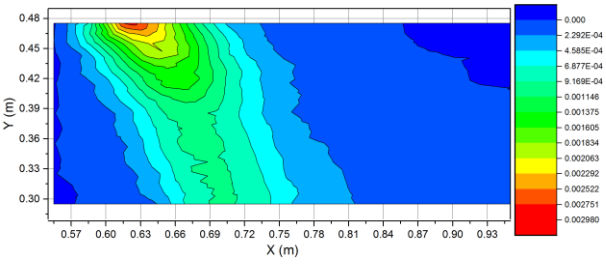

Fig. 10. Liquid film thickness (CUPID with wall shear model)

5. Conclusions

To assess the wall shear model and interfacial drag model in the CUPID1.8, the two-dimensional film flow experiment was simulated. The calculation results showed that CUPID1.8 properly predicted the behavior of liquid film flow due to the drag force by an air flow and the wall shear force by a wall. However, the quantities of local velocity vectors and the width of the liquid film showed some discrepancies. This result indicates that further improvement is required in the interfacial drag model and wall shear model to reflect the effect of the thickness of liquid film.

In addition, the effect of turbulence models for each phase and the droplet entrainment model should be evaluated simultaneously since very complicated two-phase mixing phenomena occur when the injected water encounters laterally blowing air, and forms a steady liquid film.

ACKNOWLEDGMENTS

This work was supported by National Research Foundation of Korea (NRF) grant funded by the Korea government (MSIP).

REFERENCES

[1] J. J. Jeong, et al., The CUPID code development and assessment strategy, Nuclear Engineering and Technology, Vol. 42, No. 6, 2010.

[2] H. K. Cho, et al., Recent improvements to the multi-dimensional semi-implicit two-phase flow solver, CUPID, Proceedings of the 17th International Conference on Nuclear Engineering (ICONE17), July 12-16, Brussels, Belgium, 2009.

[3] J. H. Yang, H. K. Cho, G. C. Park, Experimental Study on Two-dimensional Film Flow with Lateral Air Injection, The 10th International Topical Meeting on Nuclear Thermal-Hydraulics, Operation and Safety (NUTHOS-10), Okinawa, Japan, December, 14-18, 2014.

[4] H. Y. Yoon, et al., CUPID Code Manual Volume I: Mathematical Models and Solution Methods, Korea Atomic Energy Research Institute, KAERI/TR-4403/2011.

[5] CD-adapco, STAR-CCM+ User Guide, 2006.